

Electrospun polypyrrole-coated polycaprolactone nanoyarn nerve guidance conduits for nerve tissue engineering

Xin PAN^{1,2}, Binbin SUN (✉)¹, and Xiumei MO (✉)³

1 Department of Orthopaedics, Shanghai Ninth People's Hospital, Shanghai Jiao Tong University School of Medicine, Shanghai 200011, China

2 Sunna Technologies (Shanghai) Co., Ltd., Shanghai 201203, China

3 State Key Laboratory for Modification of Chemical Fibers and Polymer Materials, College of Chemistry, Chemical Engineering and Biotechnology, Donghua University, Shanghai 201620, China

© Higher Education Press and Springer-Verlag GmbH Germany, part of Springer Nature 2018

ABSTRACT: Nerve guidance conduits (NGCs) can provide suitable microenvironment for nerve repair and promote the proliferation and migration of Schwann cells (SCs). Thus, we developed nerve guidance conduits (NGCs) with polypyrrole-coated polycaprolactone nanoyarns (PPy-PCL-NYs) as fillers in this study. PCL-NYs with the oriented structure were prepared with a double-needle electrospinning system and then PPy was coated on PCL-NYs via the *in situ* chemical polymerization. Subsequently, PCL nanofibers were collected around nanoyarns by the conventional electrospinning process as the outer layer to obtain PPy-PCL-NY nerve guidance conduits (PPy-PCL-NY NGCs). PPy-PCL-NYs were analyzed by SEM, FTIR and XPS. Results showed that PPy was homogeneously and uniformly deposited on the surface of PCL-NY. Strain–stress curves and the Young's modulus of PPy-PCL-NYs were investigated compared with those of non-coated PCL-NYs. Studies on biocompatibility with SCs indicated that PPy-PCL-NY NGCs were more conducive to the proliferation of SCs than PCL-NY NGCs. In summary, PPy-PCL-NY NGCs show the promising potential for nerve tissue engineering repair and regeneration.

KEYWORDS: electrospinning; Schwann cell (SC); polypyrrole (PPy); polycaprolactone nanoyarn (PCL-NY); nerve guidance conduit (NGC)

Contents

| | | | |
|-----|----------------------------|-----|--|
| 1 | Introduction | 2.4 | Preparation of NGCs containing PCL-NYs and PPy-PCL-NYs |
| 2 | Materials and methods | 2.5 | Morphologies of nanoyarns and NGCs |
| 2.1 | Materials | 2.6 | Characterization |
| 2.2 | Electrospinning of PCL-NYs | 2.7 | The proliferation and infiltration of SCs on PCL-NY NGCs and PPy-PCL-NY NGCs |
| 2.3 | Fabrication of PPy-PCL-NYs | 2.8 | Statistical analysis |
| | | 3 | Results and discussion |
| | | 3.1 | Morphologies of PPy-PCL-NYs and NGCs |
| | | 3.2 | Characterization |
| | | 3.3 | Mechanical properties |

Received September 26, 2018; accepted November 7, 2018

E-mails: sunbinbin1992@163.com (B.S.), xmm@dhu.edu.cn (X.M.)

3.4 The SC proliferation in NGCs

4 Conclusions

Acknowledgements

References

1 Introduction

Peripheral nerve injury is a serious problem of clinical disease. Peripheral nerve defects and injury can cause severe loss of perception and motor dysfunction. Long distance peripheral nerve injury is sometimes difficult to self-repair. Nowadays, autologous nerve transplantation is the golden standard for the repair of nerve defects. However, the sources of the donor are limited, and there are also many drawbacks, such as neural mismatch, reoperation, loss of function of the transplant area, and neuroma [1]. Therefore, it is necessary to provide suitable tissue engineering scaffolds to promote cellular migration and axonal growth during the nerve repair. At present, most of nerve conduits used in clinic have hollow structures which cannot guide the growth of cells and axons, and during the axonal regeneration, the hollow structure of nerve conduit may cause disorder of binding sites [2–5]. Hence, it is particularly urgent to design new nerve guidance conduits (NGCs) that can provide excellent microstructure for the orientated growth of nerve cells and axons. Currently, there are many ways to prepare NGCs, such as phase separation, self-assembly, and electrospinning [2–3,6–9]. Among them, electrospinning is regarded as the most common and effective technology for tissue engineering scaffolds. Nanofibers formed by electrospinning have high specific surface area, which can simulate the structure of the extracellular matrix (ECM) and facilitate cellular adhesion, proliferation and migration. Electrospun nanofiber scaffolds have been widely used in the field of tissue engineering repair such as blood vessels, nerves, osteogenesis, skin and so on. Interestingly, nanofiber scaffolds with the oriented structure providing the “contact guidance” promote Schwann cells (SCs) unidirectional proliferation and migration, and then the special topological structure promotes axon growth without nerve growth factor treatment [6,10–11]. Lundborg et al. [12] fabricated a kind of nerve conduits, silicone tube as out layer and 8 Nylon threads placed parallel inside the conduit as filler to repair the injured nerve in rats. The results showed that the nerve defect segments were successfully repaired in rats and the axon grew along the direction of the filler. As a contrast, the axon in silicone

conduits without filler could not grow to the distal end. Yucel et al. [13] reported a kind of nerve conduits wrapping aligned micropattern film into electrospinning nerve conduits. The study demonstrated that the aligned micropattern film facilitate the migration, proliferation and survival of native cells. These results suggest that materials with the aligned structure as a filler for nerve conduit be beneficial to the directional diffusion and proliferation of cells. In previous studies, Li et al. [14] fabricated continuous poly(L-lactic acid) (PLLA) nanoyarns using a dual electrospinning system, and then constructed a nerve conduit taking PLLA nanoyarns as filler in poly(L-lactide-co-caprolactone) (PLCL) hollow nerve conduits. The research showed that the parallel arrangement of nanoyarns in the lumen contributed to the proliferation and differentiation of SCs within the nerve conduit.

In the current decades, biodegradable materials with good biocompatibility and mechanical properties have been extensively applied in nerve tissue engineering. Polycaprolactone (PCL), certified by the US Food and Drug Administration (FDA), is the biodegradable polyester that has excellent biocompatibility and mechanical properties [15]. However, due to its low hydrophilicity and lack of corresponding functional groups, PCL-based scaffolds are inadequate for cell adhesion and proliferation, which limits its repair ability. A lot of physical chemistry and surface post-processing technologies have been used to solve the problem of adhesion and proliferation of cells on the hydrophobic surface. Conductive polymer materials have been applied in tissue engineering due to their unique physical and chemical properties. In some studies, conductive materials can promote cell proliferation and migration and it also contributes to tissue regeneration and repair, especially for nerve, muscle, and heart tissue [16–17]. Polypyrrole (PPy) is one of the most stable conductive materials and compared with other ones, it has no toxicity to cells and has good biocompatibility. Furthermore, some biodegradable materials such as PCL, PLCL and silk protein after being coated with PPy show increased biocompatibility and promoted cell adhesion and proliferation. Previous studies have shown that conductive materials play a good role in the axonal growth and nerve regeneration in clinical applications [12]. The addition of conductive materials can promote the proliferation, adhesion and migration of SCs [18–22]. For example, Sun et al. [23] designed PPy-coated poly(L-lactic acid-co- ϵ -caprolactone)/silk fibroin (PLCL/SF) electrospun nanofiber scaffolds and it was found that the electrospun PLCL/

SF scaffolds not only increase the mechanical properties and improve the biocompatibility, but also retain the morphology of nanofibers. Besides, this study also showed that the PPy coating significantly promoted the SCs proliferation on PLCL/SF scaffolds.

In this study, we used double-needle electrospinning devices to prepare PCL nanoyarns (PCL-NYs) and random PCL nanofibers were produced by common electrospinning. PPy-coated PCL nanoyarns (PPy-PCL-NYs) were fabricated by the *in situ* chemical polymerization, and their morphology, structure and mechanical properties were investigated. The lumens of PCL NGCs were filled with PCL-NYs and PPy-PCL-NYs. SCs were cultured on PPy-PCL-NY NGCs and PCL-NY NGCs to evaluate the biocompatibility.

2 Materials and methods

2.1 Materials

PCL ($M_n = 80000$, IV: $1.145 \text{ dL} \cdot \text{g}^{-1}$) was purchased from Sigma. Pyrrole, iron(III) chloride (FeCl_3) and sodium paratoluenesulfonate (pTS) were purchased from Sigma (St. Louis, MO, USA). Hexafluoroisopropanol (HFIP) was acquired from Shanghai Darui Fine Chemlcai Co., Ltd. (Shanghai, China). Mouse SCs isolated from a sciatic nerve were supplied by the Institute of Biochemistry and Cell Biology, Chinese Academy of Sciences. All cells culture medium and reagents were obtained from Gibco Life Technologies Co., Ltd. (USA), unless otherwise noted.

2.2 Electrospinning of PCL-NYs

PCL-NYs were fabricated by electrospinning as previously described [14,24–25]. PCL was dissolved via the magnetic stirrer overnight in HFIP at the 10% (w/v) concentration. PCL-NYs were prepared by a specific device (TFS-700, Beijing Technova Technology Co., Ltd., China). The setup consisted of a high-speed funnel collecting and twisting nanofibers into yarns and a winder collecting yarns. Two injection pumps were fixed on both sides of the funnel, and the pushing speeds were 0.02 and 0.0032 mL/h. Two needles were separately charged with positive (+10 kV) and negative (−10 kV) high voltages. The speed of the funnel was 450 r/min and nanofibers deposited on the surface of the funnel were twisted into yarns. The winder moving horizontally was used to collect nanoyarns. The horizontal speed was 10 mm/min and the rate of rotating

was 10 r/min. Nanoyarns were placed in a vacuum drying oven at room temperature to remove residual solvents.

2.3 Fabrication of PPy-PCL-NYs

PPy-PCL-NYs were prepared by the *in situ* chemical polymerization [26]. Firstly, PCL-NYs were soaked in the pyrrole solution, followed by FeCl_3 and pTS, which were used as the oxidant and catalyst of the reaction solution (volume ratio of $V(\text{pyrrole}):V(\text{FeCl}_3):V(\text{pTS}) = 1:2:1$). The original solutions of pyrrole, FeCl_3 and pTS were prepared in advance. The whole polymerization reaction lasted for 12 h at 4°C . Finally, the samples were washed with ethyl alcohol followed by deionized water for three times, and dried in a vacuum oven for 24 h.

2.4 Preparation of NGCs containing PCL-NYs and PPy-PCL-NYs

NGCs have a special structure with nanoyarns as the filler and the random nanofiber membrane as the shell. Because of the highly-oriented structure of nanoyarns, it can induce the proliferation, adhesion, spreading and migration of nerve cells. A schematic diagram of the preparation of NGCs containing PCL-NYs and PPy-PCL-NYs was shown in Fig. 1. PCL-NYs and PPy-PCL-NYs were prepared as mentioned before [14,23–24]. Then, pre-prepared PPy-PCL-NYs were arranged in parallel on the surface of the stainless steel rod and fixed at both ends, and so were PCL-NYs. The metal rod attached with nanoyarns was used as collector, electrospinning PCL nanofibers as the tube shell layer. During the process, the electrospinning voltage was 12 kV, the flow rate was 1 mL/h and the collect distance was 15 cm. The metal rod with nanoyarns was fixed on the electric motor and the rotational speed was 5 r/min. After electrospinning for 2 h, the metal rod was removed, and NGCs filled with PPy-PCL-NYs were obtained. PCL-NY NGCs were prepared by the same method. The prepared samples were placed in a vacuum oven for 24 h, and subsequently liquid nitrogen was used to make them cool down. Finally such samples were cut into pieces 1 cm in length and stored in 5 mL vial.

2.5 Morphologies of nanoyarns and NGCs

Morphologies and structures of PCL-NYs, PPy-PCL-NYs, PCL-NY NGCs and PPy-PCL-NY NGCs were observed by scanning electron microscopy (SEM; Phenom XL,

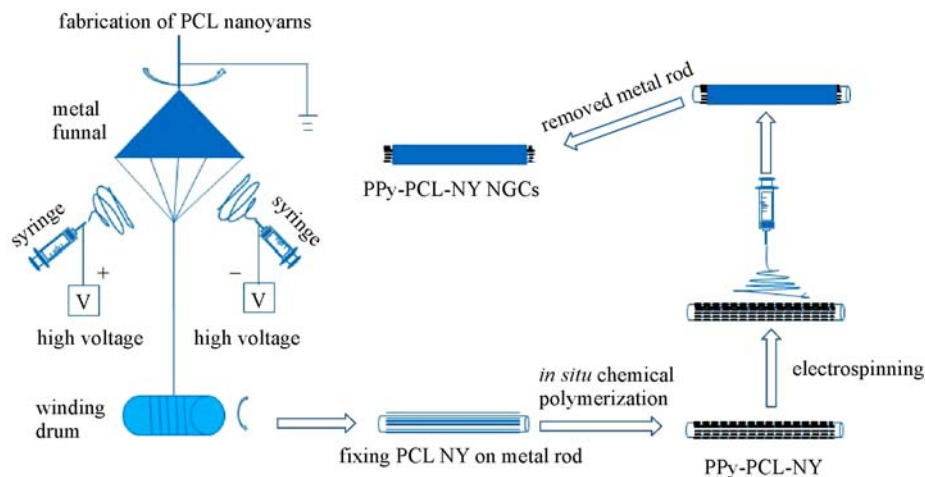


Fig. 1 Schematic diagram of PPy-PCL-NY NGCs fabrication process.

Phenom-World B.V., Netherlands). Samples were dried by a vacuum oven to remove residual solvents.

2.6 Characterization

Chemical properties of PCL-NYs and PPy-PCL-NYs were detected by Fourier transform infrared spectroscopy (FTIR; Nicolet 6700, Thermo Fisher Scientific, Inc., Waltham, MA, USA) and X-ray photoelectron spectroscopy (XPS; Thermo Scientific K-alpha, USA). As the superficial areas of nanoyarns were too small, it was inconvenient to analyze their surface chemical properties. Therefore, nanoyarns were woven into film to characterize above related properties.

Mechanical properties of PCL-NYs and PPy-PCL-NYs were tested by tensile and compression testing machine (HY-940FS, Hengyu Instrument Co., Ltd., China) at the ambient temperature 20°C and the relative humidity 65%, and the tensile rate was 10 mm/min. The parallel test on each sample was performed for five times, and stress-strain curves were drawn using Origin 9.0 software.

2.7 The proliferation and infiltration of SCs on PCL-NY NGCs and PPy-PCL-NY NGCs

SCs were used by detecting their morphology and proliferation effect on different scaffolds. SCs were cultured in Dulbecco's modification of Eagle medium (DMEM) containing 10% fetal bovine serum (FBS) and 1% double antibiotics at 37°C, 5% CO₂ and 95% humidity. The medium was changed every two days. Before cells seeding, the previously prepared NGC samples were placed in 24-well plates, each group of which was tested

with three parallel samples. The samples were sterilized with 75% alcohol, washed with phosphate buffer saline (PBS), treated by DMEM for 2 h at 37°C, and rinsed with PBS for three times. The SCs with a density of 1×10^4 were seeded into the end of each NGC, and the plate containing NGC scaffolds was cultured on a shaker (60 r/min) in the incubator. The fresh medium was changed every two days. After incubation for 1, 3, 5 and 7 d on samples, the SC proliferation was estimated on PCL-NY NGCs and PPy-PCL-NY NGCs using the MTT assay (Sigma-Aldrich Co., USA) ($n = 3$). The optical density (OD) value was measured at the wavelength of 492 nm with an enzyme labeling instrument, because the amount of the MTT crystallization was proportional to the number of cells which was further reflected by the absorbance.

To further observe the proliferation of SCs on different scaffolds, subsequent culture for 7 d was carried out. After the medium was removed, the samples were rinsed by PBS for three times, fixed with 4% paraformaldehyde for 12 h at 4°C, paraffin-embedded, cut into slices, and cleaned with PBS. After dewaxing with xylene, some scaffolds were stained with hematoxylin-eosin (HE), while others were processed with rabbit anti-S-100 antibody (1:100, Thermo Fisher Scientific, USA) overnight, and then stained with rhodamine (TRITC)-goat anti-rabbit IgG (1:200, Thermo Fisher Scientific, USA) and DAPI (1:200) for 30 and 5 min, respectively. The samples were treated with HE staining and immunofluorescence staining, which were used to determine the SC infiltration using the inverted fluorescence microscopy (IX71, Olympus, Japan) and confocal laser scanning microscopy (CLSM; C2, Nikon, Japan).

2.8 Statistical analysis

The experimental data were analyzed by Origin 9.0 (Origin Lab Inc., USA), and the results were expressed as mean \pm standard deviation (SD). Significant difference was obtained by one-way analysis of variance (ANOVA). The value of $p < 0.05$ was considered to be statistically significant.

3 Results and discussion

3.1 Morphologies of PPy-PCL-NYs and NGCs

Morphologies of PCL-NYs and PPy-PCL-NYs can be observed by digital and SEM images shown in Fig. 2. In order to avoid destroying the orientation structure and morphology of PCL-NYs, PPy was deposited on the surface of PCL-NYs by the *in situ* polymerization. The formation of the PPy coating could be judged by the color change of the nanoyarns surface. Before polymerization, PCL-NYs were white (Fig. 2(a)), while after the immersion in the reaction solution, the *in situ* polymerization caused PPy deposited on the surface of nanoyarns and turned the color black (Fig. 2(d)), indicating that PPy had been successfully coated on PCL-NYs. As can be seen from Figs. 2(b) and 2(c), PCL-NYs were composed of nanofibers with certain orientation and homogeneity. From Figs. 2(e) and 2(f), it is observed that some PPy nanoparticles were on the fiber surface of PPy-PCL-NYs and the polymerization of PPy did not destroy the structure and morphology of nanoyarns. The overall structure and morphology of PCL-NY NGCs and PPy-PCL-NY NGCs are shown in Fig. 3, from which it can be seen that dozens of PCL-NYs be in the lumen (Figs. 3(a) and 3(b)). The images of PCL-NYs and PPy-PCL-NYs in NGCs are shown in Figs. 3(c) and 3(d), respectively. Nanoyarns in the nerve conduit exhibited unidirectional arrangement, which is more conducive to the migration and proliferation of SCs than the hollow conduit.

3.2 Characterization

The coating of PPy on PCL-NYs was analyzed and verified by FTIR and XPS. FTIR results are shown in Fig. 4, from which it can be seen that both PCL-NYs and PPy-PCL-NYs had a strong absorption peak at the wavenumber of 1730 cm^{-1} corresponding to the C=O stretching vibration, while those at both 2924 and 2858 cm^{-1} corresponding to

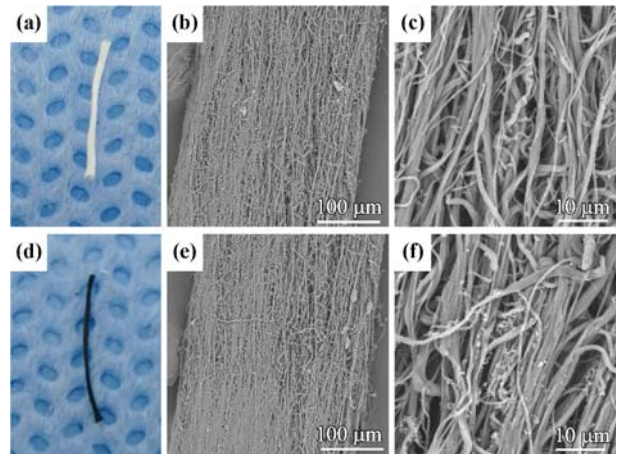


Fig. 2 Digital and SEM images of (a)(b)(c) PCL-NYs and (d)(e)(f) PPy-PCL-NYs.

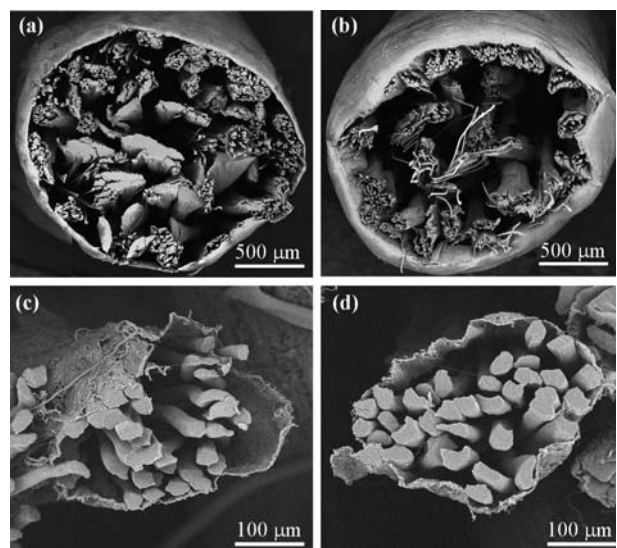


Fig. 3 SEM images of cross-sections of (a) PCL-NY NGCs, (b) PPy-PCL-NY NGCs, (c) intraductal PCL-NYs, and (d) intraductal PPy-PCL-NYs.

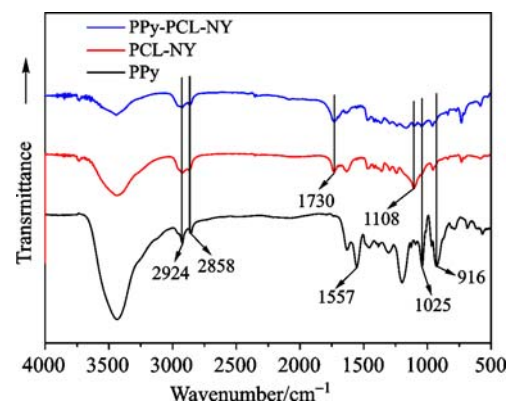


Fig. 4 FTIR spectra of PPy, PCL-NYs and PPy-PCL-NYs.

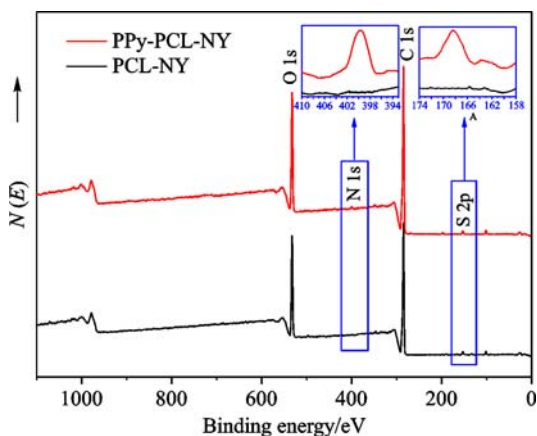


Fig. 5 XPS spectra of PCL-NYs and PPy-PCL-NYs.

Table 1 Surface elemental compositions of PCL-NYs and PPy-PCL-NYs

| Sample | c(C)/% | c(N)/% | c(O)/% | c(S)/% |
|-------------|--------|--------|--------|--------|
| PCL-NYs | 75.11 | 0.00 | 0.23 | 0.00 |
| PPy-PCL-NYs | 76.31 | 4.17 | 1.09 | 0.14 |

the $-\text{CH}_2-$ expansion vibration. For raw PPy, there were three characteristic absorption peaks at 1557, 1025 and 916 cm^{-1} . The strong absorption peaks at 1557 and 1025 cm^{-1} were mainly attributed to the stretching vibration of pyrrole rings (C–C asymmetric stretching vibration) and the bending deformation of N–H groups, respectively. The band appearance at 916 cm^{-1} , assigned to the bending deformation of C–H groups belonging to raw PPy, indicated that PPy had been successfully polymerized onto PCL-NYs. However, the characteristic peaks of PPy-PCL-NYs at 2924 and 2858 cm^{-1} showed a significant decrease, mainly due to the polymerization of PPy weakening original characteristic functional groups in PCL. XPS spectra and surface elemental compositions of both PCL-NYs and PPy-PCL-NYs are revealed in Fig. 5 and Table 1, respectively. In Fig. 5, the PCL-NYs curve revealed two absorption peaks detected at 284.6 and 533.1 eV respectively representing C 1s and O 1s, while for the PPy-PCL-NYs curve, also there were two peaks detected at 398.3 and 196.1 eV corresponding to N 1s and S 2p, respectively. In addition, the quantitative analysis on surface elemental composition was performed and results are summarized in Table 1. It reveals that the content of the N element increased from 0 (PCL-NY) to 1.09% (PPy-

PCL-NY), attributed to the introduction of pyrrole with intramolecular rings containing the N element. The additional 0.14% of the S element was detected in PPy-PCL-NYs, because pTS was added in the polymerization reaction.

3.3 Mechanical properties

In the process of tissue engineering repair, good mechanical properties can promote cell migration and growth, as well as tissue regeneration. Figure 6 reveals tensile stress–strain curves of PCL-NYs and PPy-PCL-NYs, and values of the tensile stress at break, the elongation at break and the Young's modulus of both PCL-NYs and PPy-PCL-NYs are presented in Table 2. After the coating of PPy on PCL-NYs, the tensile stress at break decreased from (76.21 ± 0.50) MPa (PCL-NYs) to (73.66 ± 0.33) MPa (PPy-PCL-NYs), while the elongation at break also decreased from $(1546.46 \pm 25.52)\%$ (PCL-NYs) to $(1004.04 \pm 5.91)\%$ (PPy-PCL-NYs). However, the Young's modulus increased from (10.55 ± 0.23) to (11.73 ± 0.05) MPa after coating owing to the brittleness of PPy.

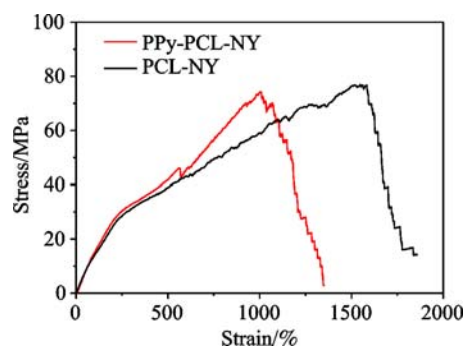


Fig. 6 Stress–strain curves of PCL-NYs and PPy-PCL-NYs.

3.4 The SC proliferation in NGCs

Ideal tissue engineering scaffolds can mimic the function of natural tissues. It is believed that nanofiber scaffolds prepared by electrospinning can simulate the environment of ECM and provide a good growth environment for cell adhesion and proliferation [27–29]. SCs can form Bunker cell bands on the surface of injured peripheral nerves, promote myelin formation, and regulate the growth and maturation of new nerve axons, playing an important role

Table 2 Mechanical properties of PCL-NYs and PPy-PCL-NYs

| Sample | Elongation at break/% | Tensile stress at break/MPa | Young's modulus/MPa |
|-------------|-----------------------|-----------------------------|---------------------|
| PCL-NYs | 1546.46 ± 25.52 | 76.21 ± 0.50 | 10.55 ± 0.23 |
| PPy-PCL-NYs | 1004.04 ± 5.91 | 73.66 ± 0.33 | 11.73 ± 0.05 |

in promoting regeneration and repair of injured peripheral nerves [30]. In this research, SCs were cultured for 1, 3, 5 and 7 d, respectively. The proliferation effects of tissue culture plate (TCP), PCL-NY NGCs and PPy-PCL-NY NGCs were detected by the MTT method. As shown in Fig. 7, there was no significant difference in the cell proliferation among TCP, PCL-NY NGCs and PPy-PCL-NY NGCs after the culture for 1 d. With the increase of the culture time, the cell proliferation on different nanofibers became distinguished. After 3, 5 and 7 d, the extent of the cell proliferation of PPy-PCL-NY NGCs was significantly greater than that of PCL-NY NGCs ($p < 0.05$). The cell proliferation rate of PPy-coated nanoyarns was higher than that of uncoated nanoyarns, indicating that PPy-coated nanoyarns had more cell affinity. It might be owing to that the mechanical stretching of oriented nanoyarns bring

mechanical stimulation to cells, leading to the cell proliferation. Moreover, the PPy coating further promoted the adhesion of nanoyarns to cells, making cells contact more compactly and enabling more cells grow inside PPy-PCL-NY NGCs.

In order to further study the proliferation of SCs in different samples, HE staining and immunofluorescence staining were performed on different samples. Figure 8 shows the infiltration of SCs in PPy-PCL-NY NGCs and PCL-NY NGCs after culture for 7 d. It could be seen that the number of SCs in PPy-PCL-NY NGCs (Figs. 8(a) and 8 (b)) is higher than that of PCL-NY NGCs (Figs. 8(c) and 8 (d)). Moreover, SCs not only grew around each nanoyarn in both PPy-PCL-NY NGCs and PCL-NY NGCs, but also filled the space between nanoyarns (indicated by red circles in Fig. 8).

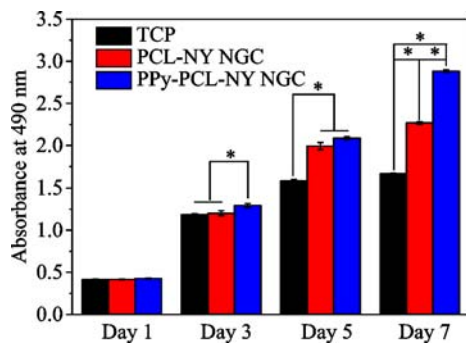


Fig. 7 MTT results of the SC proliferation on TCP, PCL-NY NGCs and PPy-PCL-NY NGCs after culturing for 1, 3, 5 and 7 d.

4 Conclusions

In this study, we prepared a new kind of NGCs with PPy-PCL-NYs as inner filler and PCL nanofibers as outer shell. PPy-PCL-NYs were prepared via the *in situ* oxidative polymerization. SEM, FTIR and XPS results confirmed that PPy nanoparticles were deposited on the surface of PCL-NYs. Compared with PCL-NYs, PPy-PCL-NYs exhibited better mechanical properties. Results from biocompatibility experiments showed that PPy-PCL-NY NGCs were more conducive to the SC proliferation than PCL-NY NGCs. Our research might provide a new direction for peripheral nerve repair or regeneration.

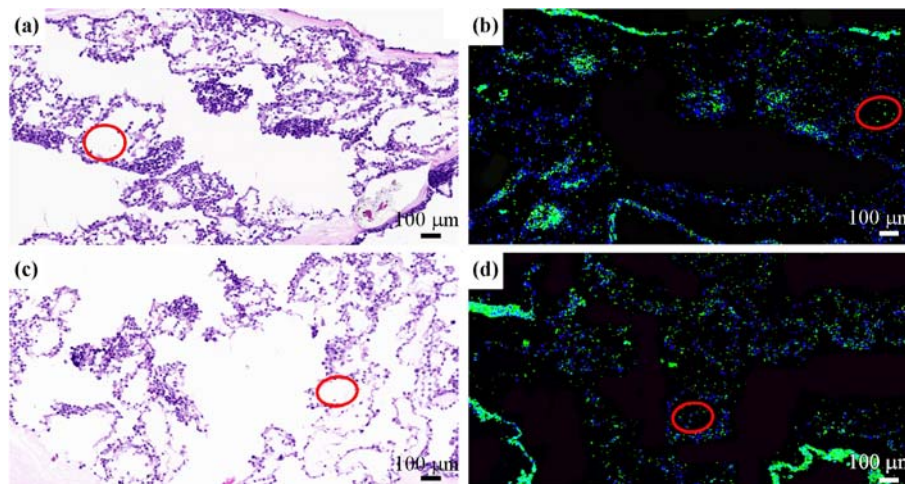


Fig. 8 (a)(c) HE images and (b)(d) immunofluorescence images with anti-S100 antibody of cross-sections after the SC culture for 7 d on PPy-PCL-NY NGCs (upper) and PCL-NY NGCs (lower).

Acknowledgements This research was supported by the National Key Research Program of China (2016YFA0201702 of 2016YFA0201700) and the National Natural Science Foundation of China (Grant Nos. 31771023 and 81802131).

References

- [1] Dvali L T, Myckatyn T M. End-to-side nerve repair: review of the literature and clinical indications. *Hand Clinics*, 2008, 24(4): 455–460
- [2] Li X, Yang Z, Zhang A, et al. Repair of thoracic spinal cord injury by chitosan tube implantation in adult rats. *Biomaterials*, 2009, 30(6): 1121–1132
- [3] Yao L, de Ruitter G C, Wang H, et al. Controlling dispersion of axonal regeneration using a multichannel collagen nerve conduit. *Biomaterials*, 2010, 31(22): 5789–5797
- [4] Ribeiro-Resende V T, Koenig B, Nichterwitz S, et al. Strategies for inducing the formation of bands of Büngner in peripheral nerve regeneration. *Biomaterials*, 2009, 30(29): 5251–5259
- [5] Tsujimoto H, Nakamura T, Miki T, et al. Regeneration and functional recovery of intrapelvic nerves removed during extensive surgery by a new artificial nerve conduit: a breakthrough to radical operation for locally advanced and recurrent rectal cancers. *Journal of Gastrointestinal Surgery*, 2011, 15(6): 1035–1042
- [6] Wang H B, Mullins M E, Cregg J M, et al. Varying the diameter of aligned electrospun fibers alters neurite outgrowth and Schwann cell migration. *Acta Biomaterialia*, 2010, 6(8): 2970–2978
- [7] Hanna A S, Son Y J, Dempsey R. Live imaging of dorsal root regeneration and the resurgence of a forgotten idea. *Neurosurgery*, 2011, 69(2): N18–N21
- [8] Xie J, MacEwan M R, Schwartz A G, et al. Electrospun nanofibers for neural tissue engineering. *Nanoscale*, 2010, 2(1): 35–44
- [9] Gelain F, Unsworth L D, Zhang S. Slow and sustained release of active cytokines from self-assembling peptide scaffolds. *Journal of Controlled Release*, 2010, 145(3): 231–239
- [10] Madduri S, Papaloizos M, Gander B. Trophically and topographically functionalized silk fibroin nerve conduits for guided peripheral nerve regeneration. *Biomaterials*, 2010, 31(8): 2323–2334
- [11] Yin Z, Chen X, Chen J L, et al. The regulation of tendon stem cell differentiation by the alignment of nanofibers. *Biomaterials*, 2010, 31(8): 2163–2175
- [12] Lundborg G, Rosen B, Dahlin L, et al. Tubular versus conventional repair of median and ulnar nerves in the human forearm: Early results from a prospective, randomized, clinical study. *The Journal of Hand Surgery*, 1997, 22(1): 99–106
- [13] Yucel D, Kose G T, Hasirci V. Polyester based nerve guidance conduit design. *Biomaterials*, 2010, 31(7): 1596–1603
- [14] Li D, Pan X, Sun B, et al. Nerve conduits constructed by electrospun P(LLA-CL) nanofibers and PLLA nanofiber yarns. *Journal of Materials Chemistry B: Materials for Biology and Medicine*, 2015, 3(45): 8823–8831
- [15] Urbanek O, Sajkiewicz P, Pierini F. The effect of polarity in the electrospinning process on PCL/chitosan nanofibres' structure, properties and efficiency of surface modification. *Polymer*, 2017, 124: 168–175
- [16] Guimard N K, Gomez N, Schmidt C E. Conducting polymers in biomedical engineering. *Progress in Polymer Science*, 2007, 32(8): 876–921
- [17] Guo B, Glavas L, Albertsson A C. Biodegradable and electrically conducting polymers for biomedical applications. *Progress in Polymer Science*, 2013, 38(9): 1263–1286
- [18] Zhang J, Qiu K, Sun B, et al. The aligned core–sheath nanofibers with electrical conductivity for neural tissue engineering. *Journal of Materials Chemistry B: Materials for Biology and Medicine*, 2014, 2(45): 7945–7954
- [19] Lee J Y, Bashur C A, Goldstein A S, et al. Polypyrrole-coated electrospun PLGA nanofibers for neural tissue applications. *Biomaterials*, 2009, 30(26): 4325–4335
- [20] Runge M B, Dadsetan M, Baltrusaitis J, et al. The development of electrically conductive polycaprolactone fumarate-polypyrrole composite materials for nerve regeneration. *Biomaterials*, 2010, 31(23): 5916–5926
- [21] Schmidt C E, Shastri V R, Vacanti J P, et al. Stimulation of neurite outgrowth using an electrically conducting polymer. *Proceedings of the National Academy of Sciences of the United States of America*, 1997, 94(17): 8948–8953
- [22] Xie J, Macewan M R, Willerth S M, et al. Conductive core–sheath nanofibers and their potential application in neural tissue engineering. *Advanced Functional Materials*, 2009, 19(14): 2312–2318
- [23] Sun B, Wu T, Wang J, et al. Polypyrrole-coated poly(l-lactic acid-co-ε-caprolactone)/silk fibroin nanofibrous membranes promoting neural cell proliferation and differentiation with electrical stimulation. *Journal of Materials Chemistry B: Materials for Biology and Medicine*, 2016, 4(41): 6670–6679
- [24] Wu T, Li D, Wang Y, et al. Laminin-coated nerve guidance conduits based on poly(l-lactide-co-glycolide) fibers and yarns for promoting Schwann cells' proliferation and migration. *Journal of Materials Chemistry B: Materials for Biology and Medicine*, 2017, 5(17): 3186–3194
- [25] Levitt A S, Knittel C E, Vallett R, et al. Investigation of nanoyarn preparation by modified electrospinning setup. *Journal of Applied Polymer Science*, 2017, 134(19): 44813
- [26] Liu P, Wu S, Zhang Y, et al. A fast response ammonia sensor

- based on coaxial PPy-PAN nanofiber yarn. *Nanomaterials*, 2016, 6 (7): E121 (10 pages)
- [27] Ichihara S, Inada Y, Nakamura T. Artificial nerve tubes and their application for repair of peripheral nerve injury: an update of current concepts. *Injury*, 2008, 39(39 Suppl 4): 29–39
- [28] Matsumoto K, Ohnishi K, Kiyotani T, et al. Peripheral nerve regeneration across an 80-mm gap bridged by a polyglycolic acid (PGA)-collagen tube filled with laminin-coated collagen fibers: a histological and electrophysiological evaluation of regenerated nerves. *Brain Research*, 2000, 868(2): 315–328
- [29] Mo X, Li D, Ei-Hamshary H A, et al. Electrospinning nanofibers for tissue engineering. *Journal of Fiber Bioengineering and Informatics*, 2013, 6(3): 225–235
- [30] Lietz M, Dreesmann L, Hoss M, et al. Neuro tissue engineering of glial nerve guides and the impact of different cell types. *Biomaterials*, 2006, 27(8): 1425–1436